Eur. Phys. J. B (2015) 88: 11
DOI: 10.1140/epjb/e2014-50448-x

THE EUROPEAN PHYSICAL JOURNAL B

Regular Article

Optical excitations of hybrid metal-semiconductor nanoparticles

Jakob Ebner, Andreas Trügler, and Ulrich Hohenester[a]

Institut für Physik, Karl-Franzens-Universität Graz, Universitätsplatz 5, 8010 Graz, Austria

Received 2 July 2014 / Received in final form 14 November 2014
Published online 12 January 2015 – © EDP Sciences, Società Italiana di Fisica, Springer-Verlag 2015

Abstract. We theoretically investigate Coulomb coupling effects in hybrid metal-semiconductor nanostructures, whose optical response is governed by plasmonic and excitonic effects (*plexcitons*). The plasmonic response of the nanoparticle is modeled within the framework of Maxwell's equations, using a suitable dielectric function for the metal, and the excitonic response is described through the Schrödinger equation and the semiconductor Bloch equations. Our approach accounts for the quantum confinement of carriers in the semiconductor, for static screening in the formation of the exciton, and for a dynamic coupling between plasmons and excitons in the optical absorption or scattering. We apply our model to a prototypical CdS-based matchstick structure and investigate the importance of the various Coulomb coupling effects.

1 Introduction

Hybrid metal-semiconductor nanostructures have recently attracted great interest [1–8] as they allow to combine the plasmonic properties of metals with the excitonic properties of semiconductors. Due to the intimate contact between the two material systems the optical response is not just a linear combination of the individual responses, but is governed by strong coupling effects, resulting in novel excitations usually referred to as *plexcitons* [5]. In the pioneering work of Zhang et al. [2], the authors demonstrated that even for the simple system of a single semiconductor quantum dot coupled to a single metallic nanosphere a rich variety of optical effects occurs, including Fano-type resonances or exciton-induced transparency [9].

From a theoretical point of view, the exciton polarizes the metallic nanoparticle, via nearfield coupling, and the polarized metallic nanoparticle couples back to the exciton, thus strongly altering its genuine optical properties [2,5,10]. This self-interaction-type coupling becomes tremendously enhanced through the plasmonic fields [11]. Hitherto, most theoretical studies have described the excitonic part through a localized dipole moment, which is a valid approximation for sufficiently small semiconductor nanoparticles. A noticeable exception is reference [6], where the authors studied a CdS-based matchstick structure with a metallic cap, and accounted for the excitonic properties within a combined Schrödinger-Maxwell description scheme. They demonstrated the importance of properly treating excitonic Coulomb coupling effects in systems where the excitonic response is not solely governed by quantum confinement effects. Similarly, in reference [12] excitons in carbon nanotubes were studied, whose wave function becomes significantly modified in presence of a nearby metallic nanoparticle.

In this paper we develop a consistent theoretical framework for excitons coupled to plasmonic nanoparticles, where the *exciton wavefunction becomes modified* by the coupling to the plasmons. In contrast to previous studies, our approach accounts for the effects of (i) quantum confinement of the electron and hole in the semiconductor; (ii) the statically screened (through the metallic nanoparticle) electron-hole Coulomb coupling in the formation of the exciton; and (iii) the dynamically screened Coulomb coupling between the exciton and the particle plasmons in the optical response.

We discuss the influence of the various Coulomb-type contributions at the example of a CdS-based matchstick structure [6], adopting an effective mass and envelope-function approach [13]. Our approach is expected to be sufficiently realistic and general to demonstrate effects relevant for state of the art hybrid metal-semiconductor nanostructures, at least in a semi-quantitative fashion. On the other hand, our approach misses a few ingredients that might be relevant for a truly quantitative comparison. First, in accordance to reference [6] we assume an abrupt metal-semiconductor interface, where the semiconductor electron and hole wavefunctions cannot penetrate into the metal. Such neglect of Schottky-type barrier effects was motivated previously [7]. We additionally neglect any kind of charging effects [6] as well as nonlocal or quantum-size effects of the dielectric response [14,15], which might be of importance for the small metallic nanospheres under investigation.

We have organized our paper as follows. In Section 2 we develop our theoretical methodology. Section 3 reports details of our numerical solution scheme within a Schrödinger-Maxwell framework. Finally, in Section 4 we

[a] e-mail: ulrich.hohenester@uni-graz.at

apply our model to a representative metal-semiconductor nanostructure, and investigate the importance of the various Coulomb coupling effects. Some details of our theoretical approach are given in the Appendices.

2 Theory

2.1 Two-level system

For conceptual clarity, we first consider the simplified situation where the semiconductor quantum dot is described through a generic two-level system, and couples via its dipole moment to a nearby metallic nanoparticle. Our approach closely follows reference [2]. In a second step, to be described below, we will account for the excitonic part of the semiconductor quantum dot in a more rigorous fashion.

Let $\sigma_{gg} = |g\rangle\langle g|$ and $\sigma_{ee} = |e\rangle\langle e|$ be the operators for the quantum dot in the ground and excited state, respectively, and $\sigma_{ge} = |g\rangle\langle e|$ the operator that promotes the dot from the ground to the excited state. The Hamiltonian for the two-level system then reads:

$$H = \Delta\sigma_{ee} - \boldsymbol{d}\cdot\left[\boldsymbol{E}^{(+)}(\boldsymbol{r}_0)\sigma_{ge} + \boldsymbol{E}^{(-)}(\boldsymbol{r}_0)\sigma_{eg}\right]. \quad (1)$$

Here Δ is the energy difference between the ground and excited state, and $\boldsymbol{d}$ is the transition dipole moment of the two-level system. The second term on the right-hand side accounts for the light-matter coupling within the dipole and rotating-wave approximations [13,16], where $\boldsymbol{E}^{(+)}(\boldsymbol{r}_0)$ is the electric field evolving with positive frequency components at the position $\boldsymbol{r}_0$ of the quantum dot. The term with $\boldsymbol{E}^{(+)}$ can be interpreted as a photon absorption with excitation of the two-level system, and the term with $\boldsymbol{E}^{(-)}$ as a photon creation upon de-excitation of the two-level system.

In references [2,12] it was shown that for a given excitation frequency ω the electric fields can be decomposed into

$$\boldsymbol{E}^{(+)}(\boldsymbol{r}_0,\omega) = \boldsymbol{E}^{(+)}_{\rm exc}(\boldsymbol{r}_0,\omega) + k^2\,\mathbb{G}(\boldsymbol{r}_0,\boldsymbol{r}_0,\omega)\cdot\boldsymbol{P}^{(+)}(\boldsymbol{r}_0,\omega), \quad (2)$$

where $\boldsymbol{E}^{(+)}_{\rm exc}$ is the electric field of the external excitation, such as a laser field, including also depolarization fields of the metallic nanoparticle. The second term accounts for a self-interaction of the quantum dot, which polarizes through its polarization $\boldsymbol{P}^{(+)} = \sigma_{eg}\boldsymbol{d}$ the metallic nanoparticle, and the induced field couples via the dyadic Green function [17] $\mathbb{G}(\boldsymbol{r}_0,\boldsymbol{r}_0,\omega)$ back to the quantum dot. k is the light wavenumber. The dyadic Green function has to be computed at the optical frequency ω using the frequency-dependent permittivities of the dielectric environment.

It is important to realize that equation (2) bridges between a quantum-mechanical description for the two-level system, described through $\boldsymbol{P}^{(+)} = \sigma_{eg}\boldsymbol{d}$, and a classical electromagnetic description for the metallic nanoparticle, described through the dyadic Green function $\mathbb{G}(\boldsymbol{r}_0,\boldsymbol{r}_0,\omega)$. We emphasize that the interplay of optical excitations of quantum dot and metallic nanoparticle, described through equations (1) and (2), introduces a wealth of interesting and nontrivial effects [2,9].

2.2 Exciton states

We next set out to develop a more general description scheme for a semiconductor quantum dot embedded in an inhomogeneous dielectric environment. This setup naturally includes hybrid semiconductor-metal nanoparticles. The strategy of our approach is to describe the optical response of the semiconductor within the usual exciton picture [13], and to lump, in the spirit of the above discussion for the two-level system, the dielectric environment (which might be governed by plasmonic effects) into an electromagnetic response formalism. To this end, we consider a Hamiltonian

$$H = H_0 + H_{\rm op} + H_{eh} + H_{ee} + H_{hh} + H_{\rm env}, \quad (3)$$

where H_0 is the single-particle Hamiltonian for electrons and holes in the semiconductor, $H_{\rm op}$ accounts for the light-induced creation of electron-hole pairs, H_{eh}, H_{ee}, H_{hh} are the Coulomb couplings between electrons and holes (we discard all Auger-type processes), and $H_{\rm env}$ describes the Coulomb coupling of electrons and holes with the dielectric environment. For simplicity, we describe in the semiconductor electrons and holes within the usual envelope-function and effective-mass approximations [13]. With the field operators $\psi^\dagger_{e,h}(\boldsymbol{r})$, which create an electron or hole at position $\boldsymbol{r}$, the effective masses $m_{e,h}$, and the confinement potentials $U_{e,h}(\boldsymbol{r})$, the single-particle Hamiltonian reads (we use Gauss and atomic units $e = m = \hbar = 1$ throughout)

$$H_0 = \sum_{i=e,h}\int \psi^\dagger_i(\boldsymbol{r})\left(-\frac{\nabla^2}{2m_i} + U_i(\boldsymbol{r})\right)\psi_i(\boldsymbol{r})\,d^3r. \quad (4)$$

Below we shall use $h_i(\boldsymbol{r}) = -\nabla^2/(2m_i) + U_i(\boldsymbol{r})$ for the single-particle Hamiltonians. We again describe the light-matter coupling within the dipole and rotating-wave approximations [13,16]

$$H_{\rm op} = -\int\left[\Omega(\boldsymbol{r})\psi^\dagger_e(\boldsymbol{r})\psi^\dagger_h(\boldsymbol{r}) + \Omega^*(\boldsymbol{r})\psi_h(\boldsymbol{r})\psi_e(\boldsymbol{r})\right]d^3r, \quad (5)$$

with the Rabi energy $\Omega(\boldsymbol{r}) = \boldsymbol{d}\cdot\boldsymbol{E}^{(+)}(\boldsymbol{r})$. Here $\boldsymbol{d}$ is the dipole moment associated with the electron-hole transition, and $\boldsymbol{E}^{(+)}(\boldsymbol{r})$ is the electric field evolving with positive frequency components. Similar to the above discussion of the two-level system, we assume that in equation (5) the electric field is the *total* field, including depolarization fields of the environment and self-interaction-like couplings of the interband polarization.

The Coulomb coupling between electrons and holes is:

$$H_{eh} = -\int G_0(\boldsymbol{r},\boldsymbol{r}')\,n_e(\boldsymbol{r})n_h(\boldsymbol{r}')\,d^3r\,d^3r', \quad (6)$$

where $G_0(\boldsymbol{r},\boldsymbol{r}') = 1/|\boldsymbol{r}-\boldsymbol{r}'|$ is the usual Coulomb interaction and $n_i(\boldsymbol{r}) = \psi_i^\dagger(\boldsymbol{r})\psi_i(\boldsymbol{r})$ denotes the particle density for electrons and holes. Similar expressions hold for electron-electron and hole-hole interactions. To account for the dielectric coupling to the environment, we decompose in the spirit of electrodynamics [18] the charge distribution into a free part $\rho_f = -n_e + n_h$, accounting for the electrons and holes in the semiconductor, and a bound part ρ_b for the polarization charges of the dielectric environment. The coupling between these charge distributions is governed by a Hamiltonian of the form

$$H_{\text{env}} = \int G_0(\boldsymbol{r},\boldsymbol{r}')\,[-n_e(\boldsymbol{r}) + n_h(\boldsymbol{r})]\rho_b(\boldsymbol{r}')\,d^3r d^3r'. \quad (7)$$

In linear response there exists a linear map between ρ_b and the free electron and hole densities $n_{e,h}$, which holds for both (quantum-mechanical) charge operators and (classical) charge densities [19]. In Appendix A we provide details for this relation, and show that the connection between ρ_b and $n_{e,h}$ is provided by the Green function G of classical electrodynamics. As densities propagate with frequencies much smaller than the optical ones, which are primarily determined by the semiconductor band gap, it is certainly a good approximation to use the static limit in the evaluation of G. We are thus led, in accordance to reference [6], to a description scheme where dielectric screening is not described as a dynamic process but already introduced at the level of the Hamiltonian of equation (6), where the Coulomb interaction $G_0(\boldsymbol{r},\boldsymbol{r}')$ is replaced by the full Green function $G(\boldsymbol{r},\boldsymbol{r}',0)/\varepsilon_0$ evaluated in the static limit, with ε_0 being the background dielectric constant of the semiconductor.

2.3 Semiconductor Bloch equations

In what follows, we describe the optical response of the semiconductor in terms of a density-matrix formalism. Owing to the special structure of the light-matter coupling of equation (5), which creates electrons and holes always pairwise, we can classify the different density matrices in powers of the electric field [20,21]. The *interband polarization* $p(\boldsymbol{r},\boldsymbol{r}') = \langle\psi_h(\boldsymbol{r})\psi_e(\boldsymbol{r}')\rangle$ is the only density matrix linear in the electric field, whereas the electron and hole distribution functions, as well as the biexciton coherence, are quadratic in $\boldsymbol{E}^{(\pm)}$. Thus, when we only consider the linear optical response, as we will do below, we keep the interband polarization and discard all higher-order density matrices. The equation of motion for p is obtained from Heisenberg's equations of motion [13,20,22], and we obtain after some simple manipulations

$$\begin{aligned} i\dot{p}(\boldsymbol{r}_e,\boldsymbol{r}_h) = &-\delta(\boldsymbol{r}_e-\boldsymbol{r}_h)\Omega(\boldsymbol{r}_e) \\ &+ [h_e(\boldsymbol{r}_e) + h_h(\boldsymbol{r}_h) \\ &- G(\boldsymbol{r}_e,\boldsymbol{r}_h,0)/\varepsilon_0]\,p(\boldsymbol{r}_e,\boldsymbol{r}_h). \end{aligned} \quad (8)$$

The first term on the right-hand side describes the creation of the interband polarization through the external light field, as well as self-interaction-like couplings of the interband polarization, with the Rabi energy

$$\Omega(\boldsymbol{r}) = \boldsymbol{d}\cdot\boldsymbol{E}_{\text{exc}}^{(+)}(\boldsymbol{r}) + k^2\int \boldsymbol{d}\cdot\mathbb{G}(\boldsymbol{r},\boldsymbol{r}',\omega)\cdot\boldsymbol{d}\,p(\boldsymbol{r}',\boldsymbol{r}')\,dr'^3. \quad (9)$$

The second term in equation (8) describes the propagation of the electron-hole pair in presence of the confinement potentials and the mutual Coulomb attraction. Equation (8) is usually referred to as the *semiconductor Bloch equation* [13,22]. In the single-particle Hamiltonians $h_i(\boldsymbol{r})$ of equation (8) one should additionally include self-interaction terms [23]

$$\begin{aligned} \Sigma(\boldsymbol{r}) &= \frac{1}{2\varepsilon_0}\lim_{\boldsymbol{r}\to\boldsymbol{r}'}\left[G\left(\boldsymbol{r},\boldsymbol{r}',0\right) - G_0\left(\boldsymbol{r},\boldsymbol{r}',0\right)\right] \\ &= \frac{1}{2\varepsilon_0}G_{\text{ind}}(\boldsymbol{r},\boldsymbol{r},0), \end{aligned} \quad (10)$$

which describe the energy change caused by the polarization of the dielectric environment. Below we will discuss how to compute the induced Green function G_{ind} in the static limit.

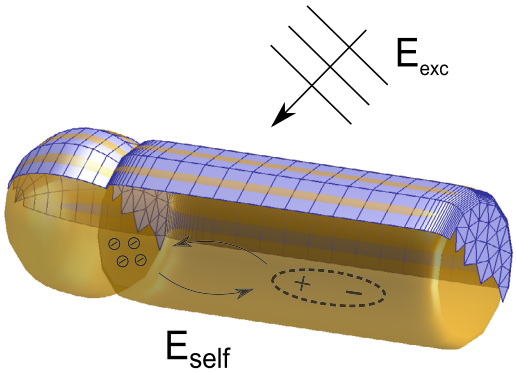

Fig. 1. Match-stick structure investigated in this work, consisting of a gold sphere (6 nm diameter) attached to a semiconductor nanorod (14 nm length). In the figure we show the boundary discretization, as used in our simulations, as well as the different Coulomb-type couplings. An external field $\boldsymbol{E}_{\text{exc}}$ excites electrons and holes (excitons) in the semiconductor, as well as surface plasmons in the metal. The electron and hole energies and states become modified through statically screened Coulomb couplings, and the exciton becomes renormalized through self-interaction-like processes governed by the dynamic interplay between the semiconductor polarization and the surface plasmon excitations. For details see text.

3 Numerical implementation

In this paper we analyze the importance of the various contributions entering the semiconductor Bloch equation of equation (8) at the example of the match-stick structure shown in Figure 1, with particle and material parameters chosen in accordance to reference [6]. Our numerical solution scheme for the optical Bloch equations can be separated into three steps: (1) calculation of the single-particle electron and hole states; (2) calculation of the

exciton states including the statically screened electron-hole Coulomb coupling; (3) solution of the optical Bloch equation of equation (8) within an exciton basis. In the following we describe all steps in more detail.

3.1 Electron and hole single-particle states

For the calculation of the electron and hole wavefunctions we assume that the carriers are fully confined within the semiconductor material, and consider a confinement potential that is zero inside the semiconductor and changes abruptly to a constant value outside the semiconductor. The semiconductor region is divided into a equidistant grid, with about hundred discretization points along the direction of the long axis, and we solve the Schrödinger equation using a finite difference scheme.

3.2 Exciton states

To compute the statically screened Coulomb interaction we employ the MNPBEM toolbox [24] for the simulation of plasmonic nanoparticles, which is based on a boundary element method approach [25]. For a given external excitation ϕ_{ext}, the solution of the Poisson equation is written down in the ad-hoc form

$$\phi(\boldsymbol{r}) = \oint_{\partial V} G(\boldsymbol{r},\boldsymbol{s})\sigma(\boldsymbol{s})\, d^2s + \phi_{\text{ext}}(\boldsymbol{r}). \tag{11}$$

Here G is the static Green function for an unbounded medium, and $\sigma(\boldsymbol{s})$ is a surface charge distribution which is chosen such that the boundary conditions of Maxwell's equations are fulfilled at the boundaries ∂V between regions of different dielectric functions [24,25]. In the limit of static screening, the metal becomes a perfect conductor that screens all fields in the inside region. Let s and m label the semiconductor and metal part, respectively. We then write the solution of the Poisson equation as:

$$\begin{aligned}\phi_s &= G_{ss}\sigma_s + G_{sm}\sigma_m + \phi_{\text{ext},s}\\ \phi_m &= G_{ms}\sigma_s + G_{mm}\sigma_m + \phi_{\text{ext},m},\end{aligned} \tag{12}$$

where we have introduced a compact notation $G\sigma$ for the boundary integral in equation (11). In the last expression of equation (12) the potential ϕ_m at the metal surface must be a constant and can be obtained from the constraint that the total surface charge $\oint \sigma(\boldsymbol{s})\, d^2s$ equals zero. As briefly discussed in Appendix B, we can obtain a linear map between σ_m and the potential $G_{ms}\sigma_s + \phi_{\text{ext},m}$, which can be inserted into the first equation of equation (12) to obtain an equation for the semiconductor surface charge. This equation can be solved along the lines presented in reference [24]. Once σ_s is known, we can compute σ_m as well as the potential everywhere else. Excitation through an external point charge allows us to determine the static Green function $G(\boldsymbol{r},\boldsymbol{r}',0)$, which enters the calculation of the excitonic states.

For the exciton states, we start from the eigenvalue problem

$$\Big(h_e(\boldsymbol{r}_e) + h_h(\boldsymbol{r}_h) - G(\boldsymbol{r}_e,\boldsymbol{r}_h,0)/\varepsilon_0 - E_\lambda\Big)\psi_\lambda(\boldsymbol{r}_e,\boldsymbol{r}_h) = 0. \tag{13}$$

Here E_λ and $\psi_\lambda(\boldsymbol{r}_e,\boldsymbol{r}_h)$ are the excitonic eigenvalues and eigenfunctions, respectively. In our computational approach we solve equation (13) by expanding ψ_λ in the basis of the confined electron and hole single-particle states, and diagonalizing the resulting Hamiltonian matrix. Throughout we assume that the exciton dipole moment is oriented along the symmetry axis of the nanostructure.

3.3 Semiconductor Bloch equations

The excitonic eigenfunctions provide a complete basis in the electron-hole subspace. In principle this basis should also include the unconfined electron and hole states, which we neglect in our approach since we are only interested in the energetically low-lying excitations close to the semiconductor bandgap. We can thus expand the interband polarization in the exciton basis

$$p(\boldsymbol{r},\boldsymbol{r}') = \sum_\lambda c_\lambda \psi_\lambda(\boldsymbol{r},\boldsymbol{r}'). \tag{14}$$

Inserting this expression into the Bloch equation (8), multiplying from the left with ψ^*_μ and integrating over the complete space, we obtain owing to the orthogonality of the excitonic states

$$(\omega + i\gamma - E_\mu)c_\mu = -\Omega_\mu - \sum_{\mu'} K_{\mu\mu'}c_{\mu'}. \tag{15}$$

We have replaced the time derivative of the interband polarization by the frequency ω of the driving laser field and have introduced a small damping constant γ to account for the finite exciton lifetime due to spontaneous emission or other environment couplings. $\Omega_\mu = \int \psi^*_\mu(\boldsymbol{r},\boldsymbol{r})\, \boldsymbol{d}\cdot \boldsymbol{E}^{(+)}_{\text{exc}}(\boldsymbol{r})\, d^3r$ is the Rabi frequency of the external laser, including depolarization effects due to dielectric surrounding of the metallic nanoparticle and the semiconductor host material. The polarization self interaction is described by the matrix

$$K_{\mu\mu'} = k^2 \int \psi^*_\mu(\boldsymbol{r},\boldsymbol{r})\, \boldsymbol{d}\cdot\mathbb{G}(\boldsymbol{r},\boldsymbol{r}',\omega)\cdot \boldsymbol{d}\, \psi_{\mu'}(\boldsymbol{r}',\boldsymbol{r}')\, d^3r d^3r'. \tag{16}$$

Note that this term introduces through the imaginary part of $\mathbb{G}$ damping effects, where the exciton decays via Ohmic losses in the metal, and also mixes the different excitonic eigenstates. This contribution, which was previously neglected [6], will be analyzed in the next section.

4 Results

For the match-stick structure shown in Figure 1 we adopt the same material parameters as used in reference [6],

Table 1. Material parameters for semiconductor as used in our simulations. m_0 is the free electron mass. For the gold dielectric function we use the data of reference [26].

Property	Value	Units
Electron mass m_e	0.21	m_0
Longitudinal hole mass m_h^z	0.22	m_0
Radial hole mass $m_h^\perp$	2.56	m_0
Bandgap	2.40	eV
Dielectric background constant	9.2	

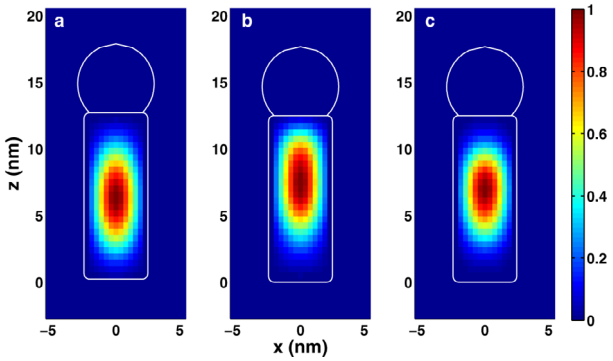

Fig. 2. Particle density for electron in arbitrary units, and for (a) electron single-particle groundstate without dielectric confinement effects, (b) electron single-particle groundstate including static polarization effects of the dielectric environment, and (c) electron density $\int |\psi_\lambda(\boldsymbol{r}_e, \boldsymbol{r}_h)|^2 \, d^3 r_h$ within Coulomb-correlated exciton groundstate, excluding the self interactions of equation (16). Density maps are normalized to their respective maxima.

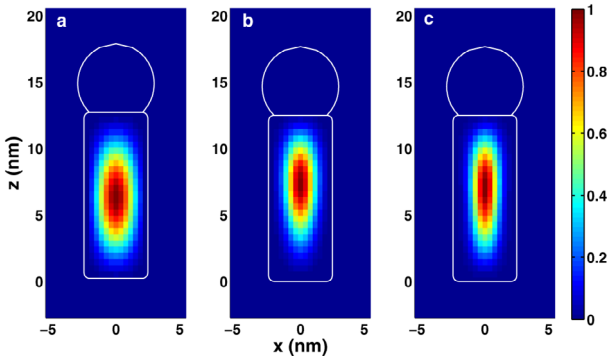

Fig. 3. Same as Figure 2 but for hole density.

which are representative for CdS as the semiconductor material and gold for the metal. The dielectric function of gold is taken from optical data [26], and the refractive index of the environment is set to 1.33. The material parameters for CdS are listed in Table 1. We assume a sharp and infinitely deep confinement potential for electrons and holes, and keep in our simulations the 20 electron and hole states of lowest energy.

Figures 2a and 3a show the electron and hole densities for the respective groundstate wavefunctions for the semiconductor confinement potential alone. When effects of the dielectric environment are included, through the image charge effects described by equation (10), the electron and

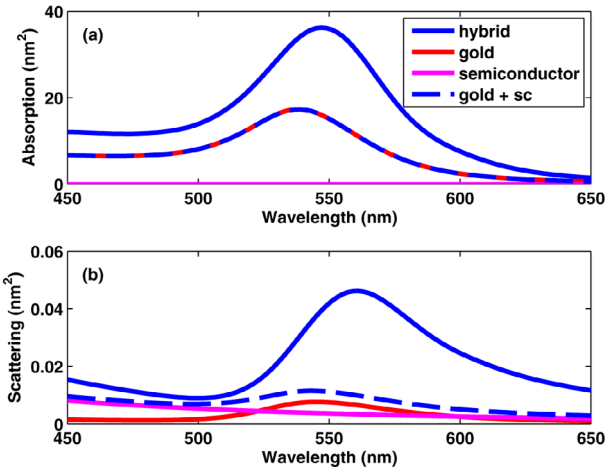

Fig. 4. (a) Absorption and (b) scattering cross sections for match-stick structure computed by neglecting excitonic features. The red and magenta lines show the contributions of the gold and semiconductor parts alone, the dashed line is the sum of the two contributions. The solid blue line shows results computed for the full hybrid structure. In all simulations the light polarization is along the symmetry axis of the matchstick structure.

hole become attracted by the metal nanoparticle as shown in Figures 2b and 3b. Finally, Figures 2c and 3c report the electron and hole densities within the statically screened exciton groundstate, where both electron and hole become slightly pushed away from the metal and semiconductor interfaces. The main reason for this somewhat unexpected behavior is the reduced electron-hole Coulomb interaction in the vicinity of the interface between the semiconductor ($\varepsilon \approx 10$) and the embedding medium ($\varepsilon \approx 1$), caused by image-charge effects. Additionally, the attractive electron-hole interaction inside the semiconductor brings the carrier wavefunctions as close as possible together, leading to a large overlap of the respective wavefunctions, as can be inferred from Figures 2c and 3c.

We next turn to the optical properties of the hybrid nanostructure under investigation. As a first approximation, in Figure 4 we report the absorption and scattering spectra obtained from simulations where the excitonic part is neglected. The red and magenta lines show results for the metal and and semiconductor part alone, whereas the blue line reports the spectra for the full hybrid structure. The optical response is governed by the plasmonic dipole peak of the gold nanosphere, around 550 nm, whereas the effect of the semiconductor (described through its background dielectric constant only) is rather weak. Comparison of the dashed line, which shows the sum of the gold and semiconductor spectra, with the solid line for the full hybrid structure already demonstrates that the optical spectra are not just sums of the metal and dielectric parts.

Things become more interesting when excitonic effects are included. Figure 5 shows the optical scattering spectra computed from the semiconductor Bloch equations. In the following we vary the strength of the semiconductor

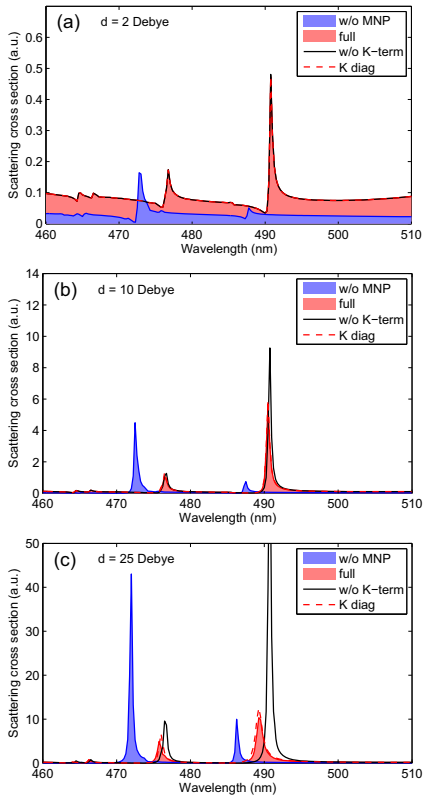

Fig. 5. Scattering cross sections for match-stick structure computed by including excitonic features, and for different dipole moment strengths. The blue filled areas report results for the semiconductor part alone, and the red areas for the full hybrid structure. We additionally plot results for simulations where the K-term of equation (16) is neglected (black solid lines) and where only the diagonal contributions $K_{\mu\mu}$ are included (red dashed lines). In all simulations we use an additional homogeneous broadening $\gamma = 1$ meV. For a discussion of the results see text.

dipole moment $\boldsymbol{d}$, which for the semiconductor nanocrystal under study is on the order of 10 Debye, in order to investigate the importance of the self-interaction term of equation (16). Let us first concentrate on the smallest dipole moment of 2 Debye, depicted in Figure 5a. The blue shaded area shows the results for the semiconductor part only. One observes a series of peaks which we assign to the various exciton excitations. When we additionally include the metallic nanocap in our simulations, see red shaded area, the peak height becomes drastically enhanced. This is because the exciton couples to the near fields of the plasmonic nanoparticle, and thus employs the plasmonic nanoantenna for a significantly enhanced light-matter coupling. The solid and dashed lines show the influence of the self-interaction term of equation (16), which is almost negligible.

For a larger dipole moment of 10 Debye, the effect of the self interaction is more pronounced. Comparing in Figure 5b the red shaded area (full simulation) with the solid line, which reports results of simulations where the K-term has been artificially neglected, one observes a significant reduction of the peak height. This is due to the additional consideration of Ohmic losses of the metal: the exciton can now decay non-radiatively by inducing an eddy current in the metal. The dashed line shows simulation results where only the diagonal part of K, which describes precisely such Ohmic lifetime effects, is included. The results almost coincide with those of the full simulation, thus indicating the importance of Ohmic losses. On the other hand, the mixing of exciton states described through the off-diagonal K-terms has practically no impact on the spectra. Only for the largest dipole moment of 25 Debye, see Figure 5c, there is a small deviation between the full simulation results and those obtained for a diagonal self interaction, which we attribute to a small exciton mixing.

Comparison of the different panels in Figure 5 shows that the plasmonic enhancement of the exciton peak decreases with increasing dipole moment, due to the increasing importance of Ohmic losses. Quite generally, plasmonic effects in gold are strongly damped above photon energies on the order of 2 eV (wavelengths below 620 nm) due to interband transitions. In this respect, it might be advantageous to investigate hybrid structures with other metal caps (e.g. silver) or for semiconductor materials with smaller band gaps.

5 Summary

To summarize, we have investigated optical properties of hybrid metal-semiconductor nanostructures. Our approach includes the quantum confinement of electrons and holes in the semiconductor, the statically screened (through the metallic nanoparticle) electron-hole Coulomb coupling in the formation of the exciton, and the dynamically screened Coulomb coupling between the exciton and the particle plasmons in the optical response. The influence of the various Coulomb-type contributions has been discussed at the example of a CdS-based match-stick structure, adopting an effective mass and envelope-function approach. For simplicity, we have refrained from including any kind of charging effects, as well as nonlocal or quantum-size effects of the dielectric response.

Our results indicate that the self-interaction of excitons with the plasmonic nanoparticle, where the exciton dynamically polarizes the metallic nanoparticle and the polarization acts back on the exciton, give rise to non-radiative decay channels due to Ohmic losses in the metal. However, for the hybrid nanoparticle under investigation mixing of exciton states is of only minor importance. We expect that the methodology developed in this work will provide a comprehensive framework for the description of excitonic states in complex dielectric environments, and will prove useful for other plexcitonic systems where the non-trivial interplay between semiconductor and metal nanoparticles leads to a number of novel effects.

This work has been supported in part by the Austrian Science Fund FWF under the SFB NextLite and by NAWI Graz.

Appendix A: Tracing out the dielectric environment

Here we show how to remove the bound polarization charges ρ_b from equation (7). As we are dealing with linear response, there exists a linear map between ρ_b and the free electron and hole densities ρ_f which holds for both (quantum-mechanical) charge operators and (classical) charge densities [19]. We start with the electric field $\boldsymbol{E}$ and dielectric displacement $\boldsymbol{D}$, which can be related to scalar potentials ϕ according to:

$$\begin{aligned} \boldsymbol{D}(\boldsymbol{r}) &= -\nabla\phi_0(\boldsymbol{r}), \quad \nabla^2\phi_0(\boldsymbol{r}) = -4\pi\,\rho_f(\boldsymbol{r}) \\ \boldsymbol{E}(\boldsymbol{r}) &= -\nabla\phi\ (\boldsymbol{r}), \quad \nabla^2\phi\ (\boldsymbol{r}) = -4\pi\,[\rho_f(\boldsymbol{r}) + \rho_b(\boldsymbol{r})]. \end{aligned} \tag{A.1}$$

The spatial extension of the nanostructure is assumed to be much smaller than the light wavelength, such that we can employ the quasistatic approximation [17], and we consider a dielectric environment described in terms of a local dielectric function $\varepsilon(\boldsymbol{r})$ evaluated at the optical frequency ω. From $\boldsymbol{D} = \varepsilon\boldsymbol{E}$ we get $\nabla\varepsilon\nabla\phi = -4\pi\rho_f$, which can be cast to the form

$$\big(\nabla^2 + e(\boldsymbol{r})\big)\phi(\boldsymbol{r}) = -4\pi\frac{\rho_f}{\varepsilon}, \tag{A.2}$$

with the operator $e(\boldsymbol{r}) = (1/\varepsilon)[\nabla\varepsilon(\boldsymbol{r})]\nabla$. For abrupt interfaces between two homogeneous dielectric materials $e(\boldsymbol{r})\phi$ then gives the induced surface charge distribution [25]. We next introduce through $\nabla^2 G_0(\boldsymbol{r},\boldsymbol{r}') = -4\pi\delta(\boldsymbol{r}-\boldsymbol{r}')$ the Green function of an unbounded medium, and through

$$\big(\nabla^2 + e(\boldsymbol{r})\big)\,G(\boldsymbol{r},\boldsymbol{r}') = -4\pi\delta(\boldsymbol{r}-\boldsymbol{r}') \tag{A.3}$$

the Green function for the inhomogeneous dielectric environment. Subtracting these two equations gives (in shorthand notation) $(\nabla^2 + e)(G - G_0) = -4\pi e G_0$, which, together with the constituting equation (A.3) for the Green function, yields a Dyson-like equation

$$G(\boldsymbol{r},\boldsymbol{r}') = G_0(\boldsymbol{r},\boldsymbol{r}') + \int G(\boldsymbol{r},\boldsymbol{r}'')e(\boldsymbol{r}'')G_0(\boldsymbol{r}'',\boldsymbol{r}')\,d^3r''. \tag{A.4}$$

Through an iterative solution one observes that also $G = G_0 + G_0 e G$ holds. We can now rewrite equation (A.2) in the form $\nabla^2\phi = -4\pi[(\rho_f/\varepsilon) + e\phi] = -4\pi[1 + eG](\rho_f/\varepsilon)$, where we have used for G the constituting equation (A.3) to arrive at the last expression. We next relate in the last expression of equation (A.1) $\nabla^2\phi$ to ρ_f, and arrive at the desired relation between the bound and free charges,

$$G_0(\boldsymbol{r},\boldsymbol{r}')\rho_b(\boldsymbol{r}') = G(\boldsymbol{r},\boldsymbol{r}')\frac{\rho_f(\boldsymbol{r}')}{\varepsilon(\boldsymbol{r}')} - G_0(\boldsymbol{r},\boldsymbol{r}')\rho_f(\boldsymbol{r}'). \tag{A.5}$$

Combining this expression with the bare electron-hole Coulomb coupling of equation (6), we see that we can replace G_0 with the screened electron hole coupling G/ε_0, where ε_0 is the background dielectric constant of the semiconductor.

Appendix B: Static screening of metal

In this Appendix we show how to express the metal surface charge in terms of the external perturbation. A related analysis can be also found in reference [27]. Our starting point is the second expression in equation (12), which can be rewritten in the form

$$\phi_m = G_{mm}\sigma_m + \tilde{\phi}_{\text{ext}}, \tag{B.1}$$

where we have used $\tilde{\phi}_{\text{ext}} = \phi_{\text{ext,m}} + G_{ms}\sigma_s$. As the metal surface is an equipotential surface, ϕ_m is constant and has to be chosen such that the total induced charge on the metal surface becomes zero, $\oint \sigma_m(\boldsymbol{s})\,d^2s = 0$. For notational simplicity we switch to a boundary element method where integrals are replaced by sums over boundary elements [24]. Then, equation (B.1) can be cast to the form

$$\sum_i \Delta a_i\,\sigma_{m,i} = \sum_{i,j}\Delta a_i\,\left(G_{mm}^{-1}\right)_{ij}\left(\phi_m - \tilde{\phi}_{\text{ext},j}\right) = 0, \tag{B.2}$$

with Δa_i being the area of the i'th boundary element. Equation (B.2) can be solved for ϕ_m and inserted into equation (B.1), which gives us the requested linear map between σ_m and the external perturbation $\tilde{\phi}_{\text{ext}}$.

References

1. T. Mokari, E. Rothenberg, I. Popov, R. Costi, U. Banin, Science **204**, 1787 (2004)
2. W. Zhang, A.O. Govorov, G.W. Brayant, Phys. Rev. Lett. **97**, 146804 (2006)
3. R. Costi, A.E. Saunders, U. Banin, Angew. Chem. Int. Ed. **49**, 4878 (2010)
4. M.B. Cortie, A.M. McDonagh, Chem. Rev. **111**, 3713 (2011)
5. A. Manjavacas, F.J. Garcia de Abajo, P. Nordlander, Nano Lett. **11**, 2318 (2011)
6. J.I. Climente, J.L. Movilla, G. Goldoni, J. Planelles, J. Phys. Chem. C **115**, 15868 (2011)
7. E. Shaviv, O. Schubert, M. Alves-Santos, G. Goldoni, R. Di Felice, F. Vallee, N. Del Fatti, U. Banin, C. Sönnichsen, ACS Nano **4712**, 4719 (2011)
8. E. Cohen-Hoshen, G.W. Bryant, I. Pinkas, J. Sperling, I. Bar-Joseph, Nano Lett. **12**, 4260 (2012)
9. R.D. Artuso, G.W. Bryant, Phys. Rev. B **82**, 195419 (2010)
10. X.W. Chen, V. Sandoghdar, M. Agio, Phys. Rev. Lett. **110**, 153605 (2013)
11. S.A. Maier, *Plasmonics: Fundamentals and Applications* (Springer, Berlin, 2007)
12. J. Waxenegger, A. Trügler, U. Hohenester, Phys. Rev. B **83**, 245446 (2011)
13. H. Haug, S.W. Koch, *Quantum Theory of the Optical and Electronic Properties of Semiconductors* (World Scientific, Singapore, 1993)
14. C. Cirarci, R.T. Hill, J.J. Mock, Y. Urzhumov, A.I. Fernandez-Dominguez, S.A. Maier, J.B. Pendry, A. Chilkoti, D.R. Smith, Science **337**, 6098 (2012)

15. T.V. Teperik, P. Nordlander, J. Aizpurua, A.G. Borisov, Phys. Rev. Lett. **110**, 263901 (2013)
16. M.O. Scully, M.S. Zubairy, *Quantum Optics* (Cambridge University Press, Cambridge, 1997)
17. L. Novotny, B. Hecht, *Principles of Nano-Optics* (Cambridge University Press, Cambridge, 2006)
18. D.J. Griffiths, *Introduction to Electrodynamics* (Pearson, San Francisco, 2008)
19. C.H. Henry, R.F. Kazarinov, Rev. Mod. Phys. **68**, 801 (1996)
20. V.M. Axt, S. Mukamel, Rev. Mod. Phys. **70**, 145 (1998)
21. U. Hohenester, Phys. Rev. B **66**, 245323 (2002)
22. F. Rossi, T. Kuhn, Rev. Mod. Phys. **74**, 895 (2002)
23. L. Hedin, S. Lundqvist, Solid State Phys. **23**, 1 (1969)
24. U. Hohenester, A. Trügler, Comput. Phys. Commun. **183**, 370 (2012)
25. F.J. Garcia de Abajo, A. Howie, Phys. Rev. B **65**, 115418 (2002)
26. P.B. Johnson, R.W. Christy, Phys. Rev. B **6**, 4370 (1972)
27. S. Corni, J. Tomasi, J. Chem. Phys. **114**, 3739 (2001)